Journal of Hazardous Materials 170 (2009) 1141–1148

Contents lists available at ScienceDirect

Journal of Hazardous Materials

journal homepage: www.elsevier.com/locate/jhazmat

Hg(II) removal from aqueous solution by bayberry tannin-immobilized collagen fiber

Xin Huang[a], Xuepin Liao[a,*], Bi Shi[b,*]

[a] Department of Biomass Chemistry and Engineering, Sichuan University, Chengdu 610065, Sichuan, PR China
[b] National Engineering Laboratory for Clean Technology of Leather Manufacture, Sichuan University, Chengdu 610065, PR China

ARTICLE INFO

Article history:
Received 13 February 2009
Received in revised form 18 May 2009
Accepted 18 May 2009
Available online 27 May 2009

Keywords:
Bayberry tannin
Collagen fiber
Immobilization
Mercury
Adsorption mechanism

ABSTRACT

A novel adsorbent was prepared by immobilizing barberry tannin (BT) onto collagen fiber, which was found effective to remove Hg(II) from aqueous solution. The bayberry tannin-immobilized collagen fiber (BTICF) shows high adsorption capacity to Hg(II) in a wide pH range of 4.0–9.0, and a maximum adsorption capacity (198.49 mg/g) was reached at pH 7.0 and 303 K when the initial concentration of Hg(II) was 200.0 mg/L. The adsorption isothermal and kinetic data were well fitted by the Langmuir equation and the pseudo-first-order rate equation, respectively. The adsorption mechanism of BTICF to Hg(II) was proved to follow a chelating reaction. The BTICF can be easily regenerated with 0.1 M lactic acid after adsorption process and recycled at least 4 times without the loss of adsorption capacity. These facts indicate that BTICF can be used as a low-cost adsorbent for effective removal of Hg(II) from aqueous solutions.

1. Introduction

Mercury is one of the most toxic heavy metals, and its existence in water would be a potential hazard to human health due to its accumulation and amplification along aquatic food chain [1]. Long term uptake of Hg(II)-contaminated water causes damage of central nervous system, impairment of kidney function, chest pain and dyspnoea [2]. Industrial and municipal wastewaters are main sources of Hg(II) contamination in natural water [3]. Therefore, it is a crucial work to remove Hg(II) from wastewater before discharge. The conventional techniques for Hg(II) removal from wastewater include precipitation [4], coagulation [5], membrane separation [6], ion-exchange [7] and adsorption [8]. Among these techniques, adsorption is the most useful and economical technique that has been widely used for the treatment of trace-Hg(II)-contaminated wastewater. Activated carbon [9], ion exchange resins [10] and other adsorbents have been used for the adsorptive removal of Hg(II) from wastewater. Nonetheless, the cost and regeneration of adsorbents are the key factors influencing their application in practice, especially for the treatment of large volume of wastewater. So, it is necessary to develop low-cost, efficient and reusable adsorbents for the adsorptive removal of Hg(II).

Recently, vegetable tannins have shown to be potential alternative for the removal of heavy metals from aqueous solution, such as lead, cadmium and chromium [11–13]. Tannins exhibit extremely high metal-binding capacity because they contain abundant adjacent phenolic hydroxyls being able to chelate with metal ions [14]. However, tannin is water-soluble compound, which restricts its practical application as an adsorbent. Therefore, great efforts have been made to overcome this disadvantage, mainly by immobilizing tannins onto various water-insoluble matrices such as agarose, hydrotalcite and cellulose [15–17]. However, these approaches are usually complicated in procedures, and tannins are still easily leaked out during adsorption process.

Collagen fiber, one of the abundant natural biomass mainly obtained from skins of domestic animals, exhibits excellent hydrophilic ability, swelling capacity and mechanical strength [18]. The functional groups of collagen fiber, including $-NH_2$, –COOH and –OH, can react with many other chemicals [19]. These facts suggest that collagen fiber would be more suitable to be used as a matrix for the immobilization of tannins. In fact, tannins have been traditionally used as tanning agents in leather industry because of their high reactivity with collagen fibers. On the basis of this principle, collagen fiber was selected as the matrix to covalently immobilize tannins through the cross-linking of aldehyde agent. The obtained adsorbents, bayberry tannin-immobilized collagen fiber (BTICF), have unique fibrous structure and excellent hydrophility, which should favor the aqueous adsorption process and thus a fast adsorption rate can be expected. Furthermore, the covalent-bond interaction between tannins and collagen fiber completely solves the problem that tannins may be leaked out during adsorption process, as compared with other tannin-immobilized approaches.

* Corresponding authors. Tel.: +86 28 85400382; fax: +86 28 85400356.
E-mail addresses: xpliao@163.com (X. Liao), shibitannin@vip.163.com (B. Shi).

0304-3894/$ – see front matter.
doi:10.1016/j.jhazmat.2009.05.086

At present work, the adsorption behaviors of BTICF to Hg(II) were investigated in order to evaluate its property as an adsorbent.

2. Materials and methods

2.1. Reagents

Collagen fiber was purchased from institute of chemical industry of forest product (China). Bayberry tannin (BT) was obtained from the barks of *myrica esculenta* by extraction with an acetone–water solution (1:1, v/v), followed by spray drying. The tannin content of the extract was 76.3%. 7-Ethylic oxazolidine, used as aldehyde cross-linking agent, was provided by Guangdong Merchandising Limited Corporation (Taiwan). $Hg(NO_3)_2{\cdot}(1/2)H_2O$ and other chemicals were all analytic reagents. The stock solution of Hg(II) (1000 mg/L) was prepared by dissolving $Hg(NO_3)_2{\cdot}(1/2)H_2O$ in deionized water, and it was diluted to an appropriate concentration when used. Diluted HNO_3 and NaOH solutions were used for adjusting the initial pH of solutions.

2.2. Preparation of BTICF

BTICF was prepared according to the procedures in our previous work [20]. In brief, 9.0 g of BT was dissolved in 300 mL of deionized water and mixed with 15.0 g of collagen fiber. Then the mixture was stirred at 298 K for 24 h. After the intermediate product was collected by filtration and washed with deionized water, 300 mL of 2% (w/w) 7-ethylic oxazolidine solution was mixed with the above product. The mixture was first stirred at 298 K for 1 h and then continuously stirred at 323 K for 4 h. Subsequently, the product was thoroughly washed with deionized water and dried in vacuum at 333 K for 12 h, and finally the BTICF adsorbent was obtained.

2.3. Experimental procedures

2.3.1. Effect of initial pH on the adsorption of Hg(II)

0.1 g of BTICF was suspended in 100 mL of Hg(II) solutions, in which the concentrations of Hg(II) were all 200.0 mg/L. The pH of the solutions was ranged from 3.0 to 9.0. The adsorption process was conducted at 303 K with constant stirring for 24 h. When the adsorption was completed, the suspension was filtered and the concentration of Hg(II) in filtrate was analyzed by Inductively Coupled Plasma Atomic Emission Spectroscopy (ICP-AES, PerkinElmer-Optima 2100 DV Model). During the analyzing process, Hg(II) is easily accumulated on the transfer tubing, spray chamber and nebulizer of the ICP-AES instrument, resulting in an inaccurate determination of Hg(II). In order to accurately determinate the concentration of Hg(II), the specific operation procedures of ICP-AES, developed by Zhu and Alexandratos [21], was adopted. According to their procedures, deionized water acidified with 1% HNO_3 was used to wash the sample introduction system and the instrument for 15–20 min after the plasma of ICP-AES was ignited. Subsequently, the Hg(II) solution was mixed with Au(III) solution and then was introduced into ICP-AES to analyze the concentration of Hg(II), where the concentration of Au(III) was fixed at 2 mg/L. After each measurement, a solution with 1 mol/L HNO_3 containing 1 mg/L Au(III) was used to wash the introduction system of ICP-AES for 3–4 min. The adsorption capacity of BTICF to Hg(II) was calculated according to the concentration difference before and after the adsorption, and was represented in units of milligram of Hg(II) per gram of adsorbent.

2.3.2. H NMR and XPS studies

In order to investigate the adsorption mechanism of BTICF to Hg(II), Proton Nuclear Magnetic Resonance (H NMR) and X-ray Photoelectron Spectrum (XPS) techniques were employed. Considering the molecular structure of BT, pyrogallic acid was used as a model compound to simulate the interaction between BT and Hg(II). The H NMR spectra of the reaction products were measured by Bruker DPX400 NMR instrument using DMSO-d_6 as solvent and TMS as an internal reference. For comparison, the H NMR analysis of pyrogallic acid was also performed. The XPS spectra of BTICF, before and after adsorbing Hg(II), were measured by VG Scientific ESCALAB-200 instrument.

2.3.3. Adsorption isotherm studies

Isotherm studies were carried out with initial concentrations of Hg(II) ranged from 50 to 1000 mg/L. The pH of the solutions was adjusted to 7.0, which is an optimal adsorption pH determined in Section 2.3.1, and the adsorption process was conducted with constant stirring for 24 h at 303 and 313 K, respectively. Then the suspension was filtered and the concentration of Hg(II) in filtrate was analyzed.

2.3.4. Adsorption kinetics studies

0.1 g of BTICF was suspended in 100 mL of Hg(II) solutions with initial concentration of 200.0 mg/L. The pH of the solutions was adjusted to 7.0. The adsorption process was conducted with constant stirring at 293, 298 and 303 K, respectively. The concentration of Hg(II) in filtrate was analyzed at a regular interval during adsorption process.

2.3.5. Effect of BTICF dose on the adsorption process

The adsorption of BTICF, at different BTICF dose, to Hg(II) was investigated with 100 mL of 200.0 mg/L Hg(II) solution in which BTICF dose varied from 0.2 to 4.0 g/L. Other experimental conditions were the same as in Section 2.3.1.

2.3.6. Effect of chloride ions on the adsorption of BTICF to Hg(II)

In view of practical application, the adsorption removal of Hg(II) in NaCl solution is an important criteria to evaluate the availability of an adsorbent due to the fact that the presence of Cl^- may change the chemical species of Hg(II) in solutions and thus may decrease the adsorption capacity of Hg(II) on the adsorbent. Herein, a series of mixture solutions of $Hg(NO_3)_2$–NaCl were prepared to investigate the effect of chloride ion on the absorption capacity of Hg(II) on BTICF, where the concentration of $Hg(NO_3)_2$ was 200.0 mg/L and NaCl concentration varied from 58.5 to 292.5 mg/L. The adsorption process was conducted at 303 K with constant stirring for 24 h. Other experimental conditions were the same as in Section 2.3.1.

2.3.7. Effect of coexisting metal ions on the adsorption of BTICF to Hg(II)

The effect of coexisting metal ions on the adsorption of BTICF to Hg(II) was investigated in the presence of Pb(II), Zn(II), Cu(II), Cd(II) and Al(III). In briefly, 0.1 g of BTICF was suspended in binary solutions of $Hg(NO_3)_2$ with $Pb(NO_3)_2$, $Zn(NO_3)_2$, $Cu(NO_3)_2$, $Cd(NO_3)_2$ or $Al(NO_3)_3$. The initial concentration of each coexisting metal ion was 200.0 mg/L. The initial pH of the solutions was adjusted to 4.0, considering the fact that some of the metal ions will precipitate at a higher pH. The adsorption was conducted at 303 K with constant stirring for 24 h. Then the suspension was filtered and the concentrations of Hg(II) and coexisting metal ions remaining in filtrate were analyzed.

2.3.8. Desorption studies

0.1 g of BTICF was used for adsorbing Hg(II) in 100 mL of Hg(II) solution (200.0 mg/L) at pH 7.0 in the same procedures as in Section 2.3.1, and then the Hg(II)-adsorbed BTICF was used for desorption experiments. Batch desorption experiments were performed using 10 mL of 0.1 M lactic acid solution with constant stirring at room

temperature for 2 h. Then the mixture was filtered and the concentration of Hg(II) in filtrate was determined, and then the desorption extent was calculated. The desorbed BTICF was re-used for adsorption test to evaluate its reusability, and the adsorption–desorption process was repeated 4 times.

2.3.9. Column adsorption

2.0 g of BTICF was soaked in deionized water for 24 h and then filled into a column with diameter of 1.10 cm and bed height of 15.00 cm. Then Hg(II) solution at 630.0 mg/L and pH 7.0 was bumped into the column at a constant velocity of 60 mL/h. Effluent was collected by an automatic collector at regular interval, and the concentration of Hg(II) in effluent was analyzed. Then the column was desorbed using 0.1 M lactic acid solution.

In this study, all the experiments were repeated at least 2 times, and the errors were found to be within 5%.

3. Results and discussion

3.1. Immobilization of bayberry tannin onto collagen fiber

Tannins are complex phenolic compounds with molecule weight ranged from 500 to 3000. According to the chemical structures of tannins, they can be divided into two major groups: hydrolysable tannins and condensed tannins [22]. BT belongs to condensed tannin and mainly consists of polymerized flavan-3-ols, as illustrated in Fig. 1. The C_6 and C_8 of A-rings of BT exhibit high nucleophilic reaction activity, which can form covalent bonds with the amino groups of collagen molecules through the cross-linking of aldehydes [23]. On the other hand, the B-ring of BT is a pyrogallol structure, which has high affinity to metal ions due to its high electrophilic reaction activities [24], and the C-ring is partly attached with galloyl groups that can improve the reaction ability of BT with metal ions like Hg(II).

The possible preparation mechanism of BTICF is presented in Fig. 1. It can be inferred that BT and collagen fibers are combined through 7-ethylic oxazolidine-formed methylene bridges, and a large number of hydrogen bonds also form between tannins, as well as tannins and collagen fibers. DSC determination (DSC, Shimadzu, DSC-60 Model) indicated that the denaturalization temperature of BTICF is 363–368 K, which is much higher than that of raw collagen fiber (333–338 K). The improved thermal stability of BTICF should be attributed to the formation of methylene bridges and a large number of hydrogen bonds.

3.2. Effect of initial pH on the adsorption of BTICF to Hg(II)

Fig. 2 shows the influence of initial pH on the adsorption capacity of BTICF to Hg(II). The adsorption capacity significantly increased to 198.49 mg/g when the pH increased from 2.0 to 4.0, and it kept almost unchanged with further pH increase. Additionally, there was no BT leaked out during adsorption process, and the pH of the solution was found to be decreased after adsorption, which indicated that protons were released into solution during adsorption process. Considering the pyrogallol structure of BTICF and the electron configuration of Hg(II) ion, it is reasonably assumed that the adsorption of BTICF to Hg(II) should follow a chelating mechanism. Hg(II) ion can act as chelating center ion to react with various electron donors due to the presence of $6s^0 6p^0$ empty orbits in its electron configuration. On the other hand, the phenolic hydroxyl of BT with lone

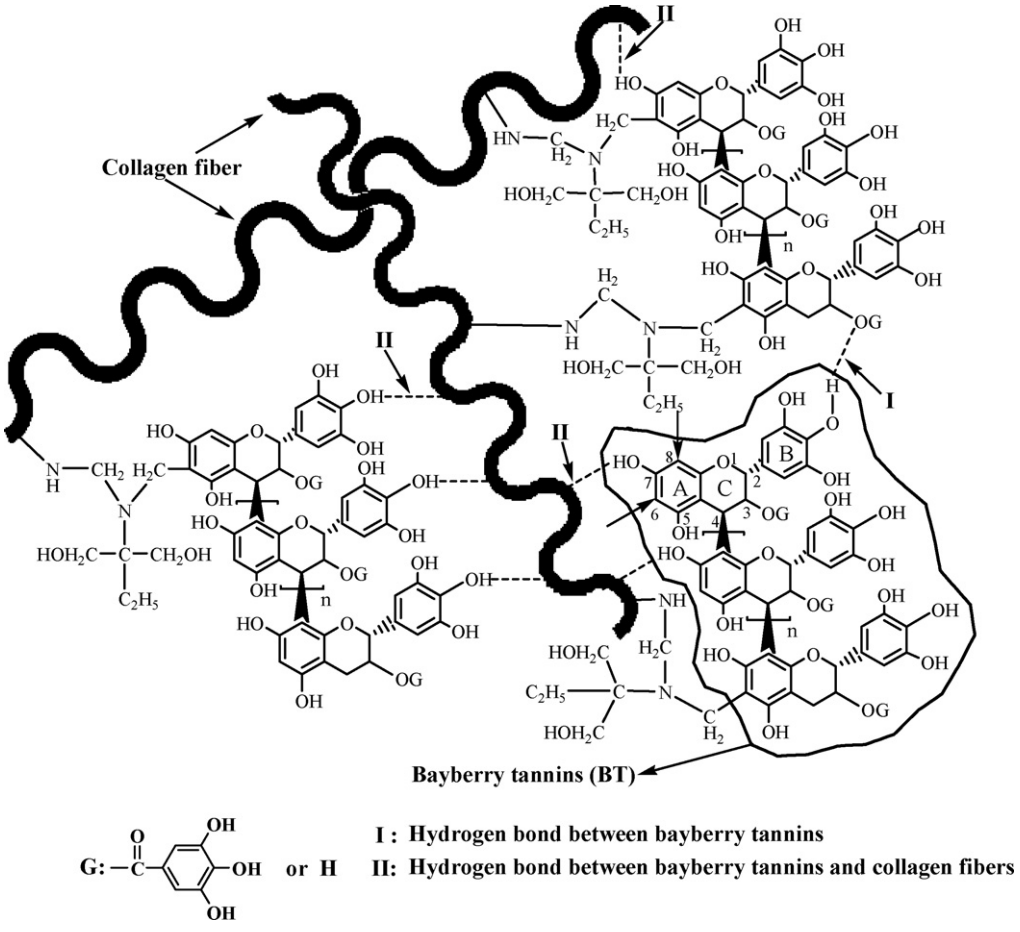

Fig. 1. Scheme of preparation mechanism of BTICF.

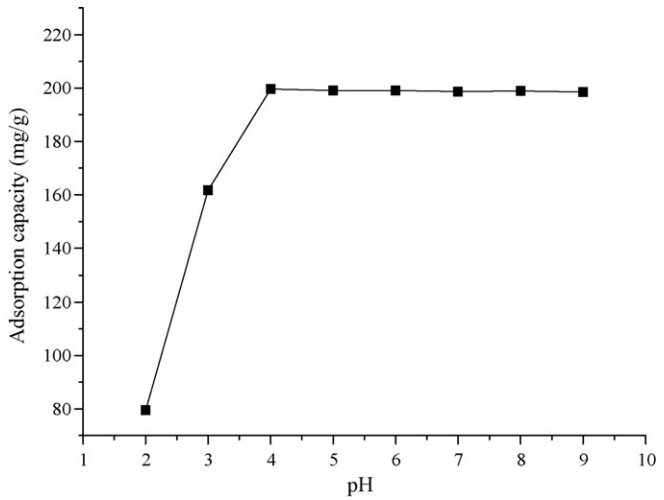

Fig. 2. Effect of initial pH on adsorption of BTICF to Hg(II) (303 K, Hg(II) = 200.0 mg/L).

pair electrons can play a role of strong donor, which has high affinity towards center metal ion. Consequently, the adsorption of BTICF to Hg(II) should consist of two steps. First, two adjacent phenolic hydroxyls of BT become negatively charged through a deprotonation process, accompanied by a release of protons into solution. Then the chelating reaction takes places, where the two charged phenolic hydroxyls act as a bidentate ligand to bond with one Hg(II) ion so as to form a five-membered chelate ring, as shown in Scheme 1. Based on this assumption, it is easy to explain the effect of pH on the adsorption capacity of BTICF to Hg(II). At low pH (2.0), BT is less active for the chelating reaction with Hg(II) ions because of the slight deprotonation of adjacent phenolic hydroxyls at high H^+ concentration. As pH increases, the deprotonation degree increases and reaches a maximum at pH 4.0, which results in a remarkable increase of the adsorption capacity. This chelating interaction can be maintained at a higher pH, so the adsorption capacity is almost unchanged in the pH range of 4.0–9.0.

According to the proposed adsorption mechanism, BT chelates Hg(II) ion by the adjacent phenolic hydroxyls in its pyrogallol structure. In order to confirm this assumption, pyrogallic acid was used as a model compound to stimulate the interaction between BT and Hg(II). The H NMR spectra of pyrogallic acid is given in Fig. 3(a). According to literatures [25,26], the peaks in the range of 8.745–8.004 ppm with integral of 3 protons are assigned to the phenolic hydroxyl protons, namely H^a and H^b. Other two peaks with integral of 3 protons, ranged from 6.434 to 6.234 ppm, are attributed to the phenyl protons of H^c and H^d, respectively. The single peak at 2.504 ppm is assigned to DMSO-d_6, and that at 3.463 ppm should belong to the proton of water remained in DMSO-d_6. Moreover, the integral assignment of protons (H^a, H^b, H^d and H^c) is very close to 2:1:2:1, which well fits the arrangement of protons in pyrogallic acid molecule.

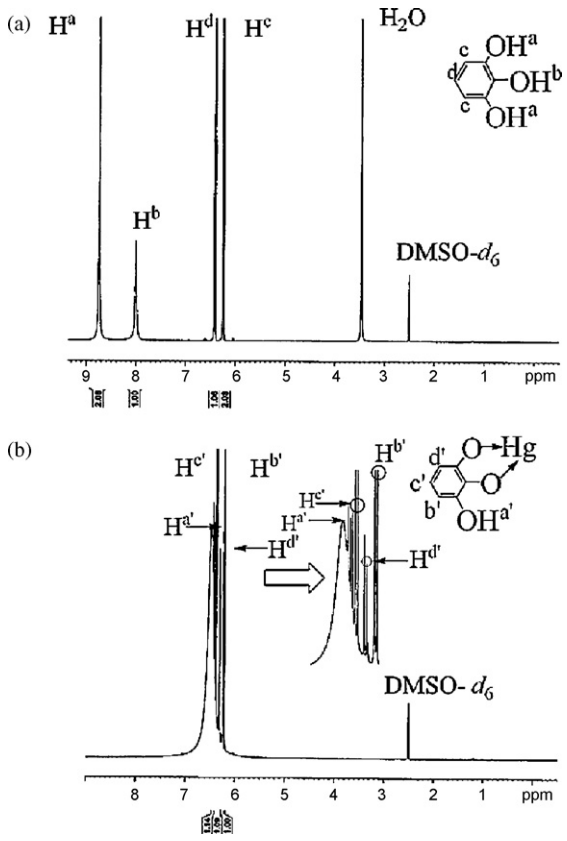

Fig. 3. H NMR spectra of pyrogallic acid (a) and pyrogallic acid-Hg(II) (b) (DMSO-d_6, 297 K, 400 MHz).

Fig. 3(b) shows the H NMR spectra of pyrogallic acid after reacting with Hg(II). The two doublets at 6.325 ppm and 6.241 ppm belong to the phenyl protons of $H^{b'}$ and $H^{d'}$, respectively, which suggests that the symmetrical geometrical structure of pyrogallic acid molecule has been destroyed due to the formation of chemical bond with Hg(II). The multiplet ranged from 6.418 to 6.378 ppm is assigned to the phenyl proton of $H^{c'}$, and its "W" arrangement is derived from the splitting effect of $H^{b'}$ and $H^{d'}$. The single peak at 6.503 ppm is assigned to the hydroxyl proton $H^{a'}$, which is not involved in the formation of complex with Hg(II) ion. Compared with Fig. 3(a), the signal of $H^{a'}$ moved to the higher field (6.503 ppm), and the signals of phenyl protons transformed from two groups to three groups. All these changes are induced by the shielding effect of Hg(II), which significantly increases the intensity of electron cloud of all protons. Most importantly, the total signal integral of protons ($H^{a'}$, $H^{b'}$, $H^{c'}$ and $H^{d'}$) indicates that only four protons in every single pyrogallic acid molecule are retained after reaction with Hg(II). In other words, the reaction ration of Hg(II) ion with phenolic hydroxyl is 1:2, which supports the assumption

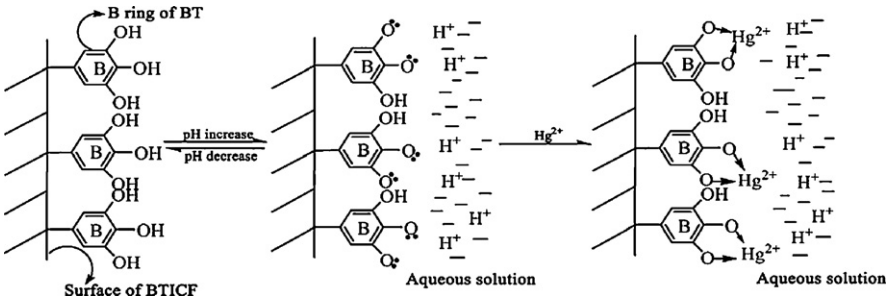

Scheme 1. Schematic graph of proposed adsorption mechanism of Hg(II) on BTICF.

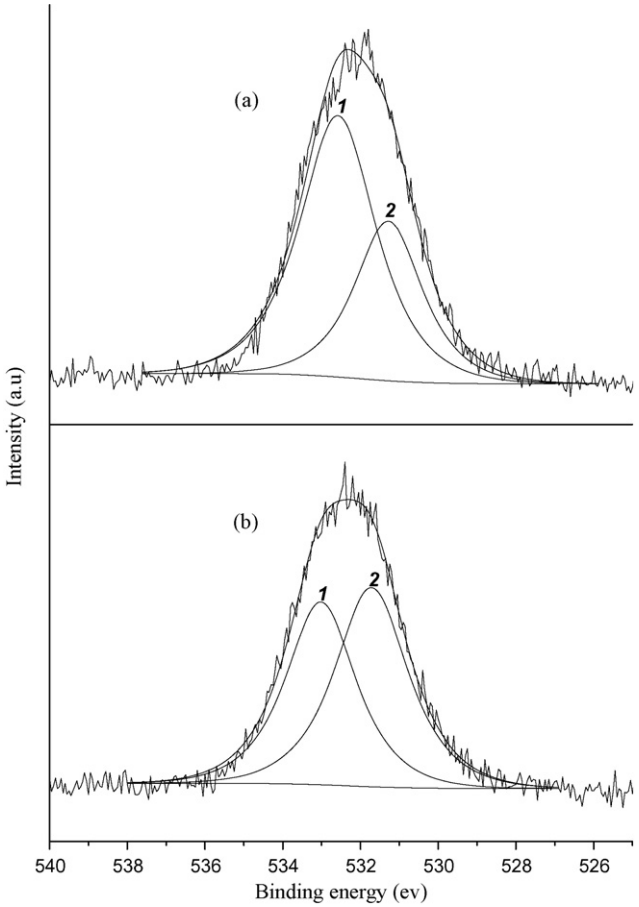

Fig. 4. The XPS O 1s spectra of BTICF (a) and BTICF–Hg(II) (b).

that Hg(II) reacts with BT by forming a five-membered chelate ring. Based on the analysis of H NMR spectra, it is proved that BT chelates Hg(II) ion through the adjacent phenolic hydroxyls in its pyrogallol structure.

Fig. 4(a) is the XPS O 1s spectra of BTICF, which contains two states of oxygen. Peak 1 at 532.7 ± 0.1 eV is assigned to the oxygen in C–O bond. Peak 2 at 531.6 ± 0.1 eV is related to the oxygen in C=O bond. The normalized intensity of peak 1 is much higher than that of peak 2. But in Fig. 4(b), the binding energy of peak 1 increases to 533.0 ± 0.1 eV and its normalized intensity dramatically decreases. Meanwhile the binding energy of peak 2 is almost unchanged (531.7 ± 0.1 eV) and its relative fraction is even higher than that of peak 1. All these facts suggest that the adsorption of Hg(II) on BTICF mainly affects the binding energy of oxygen atom in C=O bond of BT molecule. When the adsorption takes place, the adsorbed Hg(II) ions significantly decrease the electronic density around oxygen atom involved in the adsorption. Then, the C–O bond of phenolic hydroxyl in BT is affected, resulting in the change of binding energy and relative fraction of peak 1. The results obtained from XPS spectra are consistent with the conclusion of H NMR analysis. Therefore, it can be concluded that the adsorption of BTICF to Hg(II) should base on a chelating reaction, accompanied by a deprotonation process of the adjacent phenolic hydroxyls of BT, as shown in Scheme 1.

3.3. Adsorption isotherms

As shown in Table 1, the adsorption capacity of BTICF to Hg(II) is remarkable. The adsorption capacity is high up to 619.78 mg/g at 303 K when the initial concentration of Hg(II) is 997.5 mg/L,

Table 1
Isotherm model constants and correlation coefficients (R^2) for the adsorption of BTICF to Hg(II).

T (K)	$q_{e,exp.}$ (mg/g)	Langmuir fitting			Freundlich fitting		
		$q_{e,cal.}$ (mg/g)	b	R^2	k	n	R^2
303	619.78	622.31	0.071	0.98	114.3	3.12	0.92
313	643.11	645.21	0.094	0.98	134.7	3.31	0.91

$q_{e,exp.}$, $q_{e,experiment}$; $q_{e,cal.}$, $q_{e,calculation}$.

which reveals the great potential of BTICF to be used in treating Hg(II)-contaminated wastewater. In addition, the adsorption capacity increases with the increase of temperature, suggesting that the adsorption of BTICF to Hg(II) is an endothermic process in nature [27].

Adsorption isotherm data were further analyzed by the Langmuir and Freundlich models. In general, there is no theoretical model to describe the adsorption isotherms of liquid adsorption. The adsorption isotherm models used in gas adsorption are always used to describe the liquid adsorption. Langmuir model is often used for monolayer adsorption occurred on a homogeneous surface with identical adsorption sites, which can be expressed by the following equation [28]:

$$q_e = \frac{q_{\max} b C_e}{(1 + bC_e)} \quad (1)$$

where C_e and q_e are the Hg(II) concentration (mg/L) and the adsorption capacity (mg/g) of BTICF at equilibrium, $q_{\max}$ and b are the maximum adsorption capacity (mg/g) and Langmuir constant relating to the strength of adsorption, respectively. The empirical Freundlich model is appropriate for the adsorption occurred on a heterogeneous surface, which can be expressed by the following equation [29]:

$$q_e = k{C_e}^{1/n} \quad (2)$$

where C_e and q_e are the same as shown in Eq. (1), k and n are the Freundlich constants, which give an indication of the adsorption capacity and the favorability of the adsorbent, respectively.

Table 1 lists the Langmuir and the Freundlich constants and the correlation coefficients (R^2). The adsorption isotherm is well described by using the Langmuir equation with correlation coefficient higher than 0.98. In addition, the adsorption capacity (622.31 mg/g) calculated by the Langmuir equation is close to that determined by experiment (619.78 mg/g). Therefore, it is more proper to use the Langmuir model to describe the adsorption isotherms of Hg(II) on BTICF. In Section 3.1, it has been proved that Hg(II) ions are chemically adsorbed on BTICF via a chelating mechanism. BT is mainly immobilized on the surface of collagen fiber. Thus, it is reasonable to predict that Hg(II) may be adsorbed in the form of monolayer coverage on the surface of BTICF.

3.4. Kinetic studies

Kinetic studies were carried out at different temperature (293, 298 and 303 K) and the experimental results are presented in Fig. 5. It is evident that the adsorption is very fast during the first 60 min, and the adsorption equilibrium was attained in about 180 min. BTICF is in fiber state and its specific surface area is limited (2.0–6.0 m^2/g), in comparison with porous adsorbents. Therefore, it can be inferred that the BT immobilized on collagen fiber is mainly located at the outer surface and thus the diffusion resistance of mass transfer during adsorption process would be neglectable, which results in a fast adsorption process.

The adsorption kinetic data were further analyzed using a pseudo-first-order rate model (3), a pseudo-second-order rate

Table 2
Kinetics model constants and correlation coefficients (R^2) for the adsorption of BTICF to Hg(II).

T (K)	$q_{e,exp.}$ (mg/g)	Pseudo-first-order rate model			Pseudo-second-order rate model			Intraparticle diffusion model	
		$q_{e,cal.}$ (mg/g)	$k_1 \times 10^3$	R^2	$q_{e,cal.}$ (mg/g)	$k_2 \times 10^4$	R^2	k_i	R^2
293	192.1	194.3	26.4	0.99	240.3	1.07	0.99	16.68	0.94
298	195.9	197.4	27.4	0.99	243.3	1.12	0.99	17.10	0.93
303	198.5	200.2	28.7	0.99	241.5	1.28	0.99	17.53	0.93

$q_{e,exp.}$, $q_{e,experiment}$; $q_{e,cal.}$, $q_{e,calculation}$.

model (4) and an intraparticle diffusion model (5) [30,31]:

$$\log(q_e - q_t) = \log q_e - \frac{k_1}{2.303}t \quad (3)$$

$$\frac{t}{q_t} = \frac{1}{k_2 q_e^2} + \frac{1}{q_e}t \quad (4)$$

$$q_t = k_i t^{0.5} \quad (5)$$

where q_e and q_t are the amount of Hg(II)-adsorbed (mg/g) at equilibrium and at time t (min) respectively, and k_1, k_2 and k_i are the rate constants of the pseudo-first-order-rate model (min^{-1}), pseudo-second-order rate model (mg/g min) and intraparticle diffusion rate model (mg/g $min^{-0.5}$), respectively.

The "pseudo-first" and "pseudo-second" order models are macroscopic kinetic models commonly used for describing adsorption process, which suggest that the adsorption process can be considered as the "first" or "second" order chemical reaction process when the adsorption is rate-controlled step and the resistance of intraparticle diffusion can be neglected [31]. As for intraparticle diffusion model, it is used to describe the adsorption process where the intraparticle diffusion resistance is the rate-controlled step [32]. This model is particularly suitable for the description of an adsorption process when porous adsorbents, such as activated carbon, are used because they are abundance of micropores or mesopores.

Table 2 lists parameters obtained from the three models. The intraparticle diffusion rate model provides low correlation coefficient (R^2), which suggests that the Hg(II) adsorption is not an intraparticle-diffusion-controlled process. The correlation coefficients (R^2) for the pseudo-first-order rate model and the pseudo-second-order rate model are both higher than 0.99. However, only the theoretical adsorption capacity predicted by the pseudo-first-order rate model is mostly consistent with experimental data. So, the pseudo-first-order rate model is more appropriate to describe the adsorption kinetics of BTICF to Hg(II), and this reveals that the adsorption process is a rate-controlled process [33]. Moreover, the adsorption of BTICF to Hg(II) is a liquid–solid adsorption process based on external mass transfer. Therefore, it could be predicted that the rate-controlled step involved in the adsorption process might be the external mass transfer resistance and the chelating reaction occurred on the outer surface of BTICF.

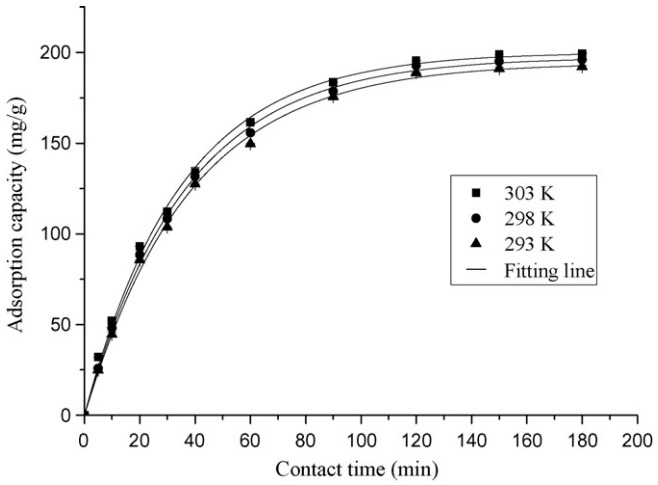

Fig. 5. The adsorption kinetics of BTICF to Hg(II) (Hg(II) = 200.0 mg/L, pH 7.0).

3.5. Effect of BTICF dose on adsorption process

Table 3 shows the effect of adsorbent dose on the removal extent of Hg(II). The removal extent of Hg(II) in solution increased from 32.38 to 98.34% as BTICF dose increased from 0.2 to 1.0 g/L, then maintained at the level when the dose was further increased to 4.0 g/L. The higher Hg(II) removal extent at larger adsorbent dose can be attributed to the availability of more adsorption sites and more surface area of BTICF. However, the adsorption capacity of BTICF to Hg(II) sharply decreases with the increase of BTICF dose For example, the adsorption capacity of Hg(II) on BTICF decreased to 49.6 mg/g when the dose of BTICF was 4.0 g/L. The lower adsorption capacity at larger adsorbent dose should be due to the overlapping of adsorption sites on the surface of BTICF [34].

3.6. Effect of chloride ions the adsorption of BTIBT to Hg(II)

It is well known that chloride ions can form stable anionic complexes with Hg(II), such as $HgCl_3^-$ and $HgCl_4^{2-}$, and their formation constants are 1.6×10^{14} and 1.25×10^{15}, respectively [35]. This implies that the presence of chloride ions might affect the adsorption of BTICF to Hg(II) because of the great affinity of chloride ion to Hg(II). Therefore, it is necessary to investigate the Hg(II)-adsorption behavior of BTICF in the presence of Cl^-. As shown in Table 4, the

Table 3
Effect of BTICF dose on the adsorption process(303 K, Hg(II) = 200.0 mg/L, pH 7.0).

Dose (g/L)	Removal extent (%)	Adsorption capacity (mg/g)
0.2	32.39 ± 0.42	326.45 ± 4.24
0.4	64.86 ± 0.36	326.90 ± 1.84
0.6	88.23 ± 0.31	296.43 ± 1.04
0.8	94.19 ± 0.02	237.36 ± 0.04
1.0	98.34 ± 0.15	198.25 ± 0.30
2.0	98.29 ± 0.22	99.07 ± 0.22
3.0	98.49 ± 0.04	66.18 ± 0.03
4.0	98.43 ± 0.05	49.61 ± 0.02

Table 4
Effect of chloride ions on the adsorption of BTICF to Hg(II).

Conc. of NaCl (mg/L)	Initial conc. of Hg(II) (mg/L)	Final conc. of Hg(II) (mg/L)	Adsorption capacity (mg/g)
0	200.0	1.51 ± 0.04	198.49 ± 0.04
58.5	200.0	9.34 ± 0.52	190.66 ± 0.52
117.0	200.0	17.10 ± 0.24	182.9 ± 0.24
175.5	200.0	24.14 ± 0.71	175.86 ± 0.71
234.0	200.0	30.30 ± 0.53	169.7 ± 0.53
292.5	200.0	107.12 ± 0.71	92.88 ± 0.71

conc., concentration.

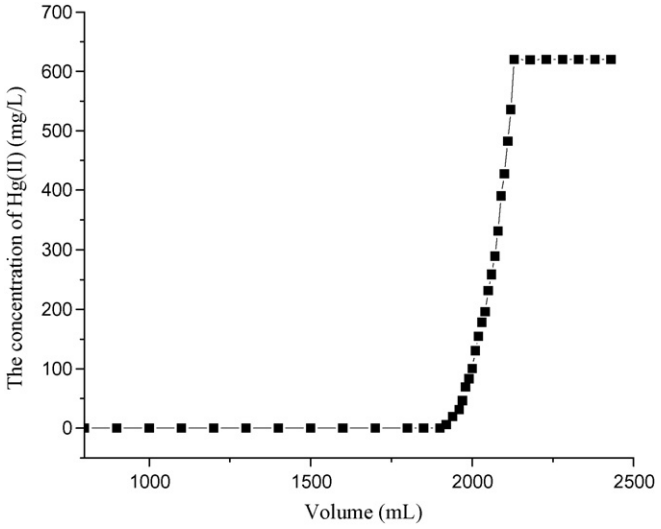

Fig. 6. Breakthrough curve of Hg(II) on BTICF column (303 K, Hg(II) = 620.0 mg/L, BTICF = 2.0 g).

adsorption capacity of BTICF to Hg(II) gradually decreases as the increase of NaCl concentration, indicating a competition between chloride ions and BTICF to combine with Hg(II). According to literature [36], ions that form outer-sphere surface complexes show decrease in adsorption with increase of ionic strength in solution. In fact, the chelating reaction occurred between Hg(II) and the adjacent phenolic hydroxyls of BT on BTICF should lead to an outer-sphere complex since the electron configuration of Hg(II) ion is $6s^0 6p^0$.

In this study, the adsorption capacity of Hg(II) on BTICF is still significant (92.88 mg/g) even the concentration of NaCl is as high as 292.5 mg/L. Therefore, the practical application of BTICF for the removal of Hg(II) from NaCl-containing wastewaters can be expected.

3.7. Effect of coexisting metal ions on the adsorption of BTIBT to Hg(II)

It was found that coexisting metal ions did not affect the adsorption of Hg(II) in solution. The adsorption capacity of BTICF to Hg(II) was around 196.00 mg/g in the presence of Pb(II), Zn(II), Cu(II), Cd(II) or Al(III), which is nearly the same as that occurred in the absence of the metal ions. The adsorption capacity of BTICF to Hg(II) did not change even it adsorbed 20.0 mg of copper per gram, and no significant adsorption was found for other coexisting metal ions. These facts suggest that BTICF is able to selectively adsorb mercury in aqueous solution to some extent, at least in the presence of the coexisting metal ions investigated.

3.8. Desorption studies

It was found that lactic acid is effective for the desorption of Hg(II) from BTICF. In batch experiments, the Hg(II)-adsorbed on BTICF can be completely desorbed by only 10 mL of 0.1 M lactic acid solution, and the Hg(II) content in desorption solution was 10 times concentrated, in comparison with that in original solution. Additionally, the desorbed BTICF can be recycled 4 times without the loss of adsorption capacity to Hg(II) (data not shown), which reveals its great potential to be used as low-cost and reusable adsorbent for the removal of Hg(II) from wastewater.

3.9. Column adsorption

Fig. 6 is the breakthrough curve of Hg(II) on BTICF column. It can be seen that about 1960 mL of Hg(II) solution (630 mg/L) passed through the column before breakthrough point, which corresponds to the adsorption capacity of 617.4 mg/g. This adsorption capacity is very close to that obtained in the isothermal studies (619.78 mg/g). The BTICF column was then desorbed with 0.1 M lactic acid. It was found that more than 98% of Hg(II) was desorbed from the BTICF column. These facts imply that the extremely effective adsorption performance of BTICF to Hg(II) can be expected in industrial application.

4. Conclusions

The adsorbent BTICF can be easily prepared by immobilizing bayberry tannin onto collagen fiber, and no BT is leaked out during the adsorption process to Hg(II). BTICF exhibits high adsorption capacity to Hg(II) in a wide pH range of 4.0–9.0, and it retains significant adsorption capacity even in the presence of high concentration of Cl^-. The adsorption of BTICF to Hg(II) follows a chelating mechanism between Hg(II) and the adjacent phenolic hydroxyls of BT on the adsorbent. BTICF is easily desorbed using 0.1 M lactic acid after the adsorption process, and it can be recycled at least 4 times without the loss of adsorption capacity to Hg(II). The excellent adsorption and desorption behaviors observed are due to the facts that BTICF is in fiber state and BT is located at the outer surface of collagen fiber. As a kind of low-cost, high effective and reusable adsorbent, the practical application of this novel adsorbent for the removal of Hg(II) from aqueous solution can be expected.

Acknowledgements

We acknowledge the financial supports provided by National Technologies R&D Program (2006BAC02A09), National Natural Science Foundation of China (20776090) and The Key Program of National Science Fund of China (20536030).

References

[1] J.E.S. Uria, A. Sanz-Medel, Inorganic and methyl mercury speciation in environmental samples, Talanta 47 (1998) 509–524.
[2] R. Say, E. Birlik, Z. Erdemgil, A. Denizli, A. Ersoz, Removal of mercury species with dithiocarbamate-anchored polymer/organosmectite composites, J. Hazard. Mater. 150 (2008) 560–564.
[3] H. Von Canstein, Y. Li, K.N. Timmis, W.D. Deckwer, I. Wagner-Döbler, Removal of mercury from chloralkali electrolysis wastewater by a mercury-resistant *Pseudomonas putida* strain, Appl. Environ. Microbiol. 65 (1999) 5279–5284.
[4] M.M. Matlock, B.S. Howerton, D.A. Atwood, Chemical precipitation of heavy metals from acid mine drainage, Water Res. 36 (2002) 4757–4764.
[5] Y. Terashima, H. Ozaki, M. Sekine, Removal of dissolved heavy metals by chemical coagulation, magnetic seeding and high gradient magnetic filtration, Water Res. 20 (1986) 537–545.
[6] A. Oehmen, R. Viegas, S. Velizarov, M.A.M. Reis, J.G. Crespo, Removal of heavy metals from drinking water supplies through the ion exchange membrane bioreactor, Desalination 199 (2006) 405–407.
[7] D. Kratochvil, B. Volesky, Biosorption of Cu from ferruginous wastewater by algal biomass, Water Res. 32 (1998) 2760–2768.
[8] B.S. Inbaraj, N. Sulochana, The role of sorption and bacteria in mercury partitioning and bioavailability in artificial sediments, J. Hazard. Mater. 133 (2006) 283–290.
[9] F.S. Zhang, J.O. Nriagu, H. Itoh, Mercury removal from water using activated carbons derived from organic sewage sludge, Water Res. 39 (2005) 389–395.
[10] S. Chiarle, M. Ratto, M. Rovatti, Mercury removal from water by ion exchange resins adsorption, Water Res. 34 (2000) 2971–2978.
[11] X. Zhan, A. Miyazaki, Y. Nakano, Mechanisms of lead removal from aqueous solutions using a novel tannin gel adsorbent synthesized from natural condensed tannin, J. Chem. Eng. Jpn. 34 (2001) 1204–1210.
[12] G. Vazquez, J. Gonzalez-Alvarez, S. Freire, M. Lopez-Lorenzo, G. Antorrena, Removal of cadmium and mercury ions from aqueous solution by sorption on treated *Pinus pinaster* bark: kinetics and isotherms, Bioresour. Technol. 82 (2002) 247–251.

[13] Y. Nakano, K. Takeshita, T. Tsutsumi, Adsorption mechanism of hexavalent chromium by redox within condensed-tannin gel, Water Res. 35 (2001) 496–500.
[14] H. Yamaguchi, R. Higasida, M. Higuchi, I. Sakata, Adsorption mechanism of heavy-metal ion by microspherical tannin resin, J. Appl. Polym. Sci. 25 (1992) 1463–1472.
[15] A. Nakajima, T. Sakaguchi, Recovery of uranium by tannins immobilized on agarose, J. Chem. Tech. Biotechnol. 40 (1987) 223–232.
[16] T.S. Anirudhan, P.S. Suchithra, Synthesis and characterization of tannin-immobilized hydrotalcite as a potential adsorbent of heavy metal ions in effluent treatments, Appl. Clay Sci. 42 (2008) 214–223.
[17] I. Chibata, T. Tosa, T. Mori, T. Watanabe, N. Sakata, Immobilized tannins-a novel adsorbent for protein and metal ion, Enzyme Microb. Technol. 8 (1986) 130–136.
[18] R.X. Liu, J.L. Guo, H.X. Tang, Adsorption of fluoride, phosphate, and arsenate ions on a new type of ion exchange fiber, J. Colloid Interf. Sci. 248 (2002) 268–274.
[19] F.H. Silver, J.W. Freeman, G.P. Seehra, Collagen self-assembly and the development of tendon mechanical properties, J. Biosci. 36 (2003) 1529–1553.
[20] X.P. Liao, M.N. Zhang, B. Shi, Collagen-fiber-immobilized tannins and their adsorption of Au(III), Ind. Eng. Chem. Res. 43 (2004) 2222–2227.
[21] X.P. Zhu, S.D. Alexandratos, Determination of trace levels of mercury in aqueous solutions by inductively coupled plasma atomic emission spectrometry: elimination of the memory effect, Microchem. J. 86 (2007) 37–41.
[22] M. Ozacar, A. Sengil, Effectiveness of tannins obtained from valonia as a coagulant aid for dewatering of sludge, Water Res. 34 (2000) 1407–1412.
[23] X.M. Zhan, X. Zhao, Mechanism of lead adsorption from aqueous solutions using an adsorbent synthesized from natural condensed tannin, Water Res. 37 (2003) 3905–3912.
[24] M. Ozacar, C. Soykan, I.A. Sengil, J. Appl. Polym. Sci. 102 (2006) 786–797.
[25] G. Aridoss, S. Balasubramanian, P. Parthiban, S. Kabilan, Studies on synthesis, characterization, and metal adsorption of mimosa and valonia tannin resins, Spectrochim. Acta A 68 (2007) 1153–1163.
[26] J.M. Seco, E. Quinoa, R. Riguera, The assignment of absolute configuration by NMR, Chem. Rev. 108 (2004) 17–117.
[27] T.S. Anirudhan, L. Divya, M. Ramachandran, Mercury(II) removal from aqueous solutions and wastewaters using a novel cation exchanger derived from coconut coir pith and its recovery, J. Hazard. Mater. 157 (2008) 620–627.
[28] I. Langmuir, The constitution and fundamental properties of solids and liquids, J. Am. Chem. Soc. 38 (1916) 2221–2295.
[29] H.M.F. Freundlich, Tiber die adsorption in losungen, Z. Phys. Chem. 57 (1906) 385–470.
[30] M.S. Chiou, H.Y. Li, Adsorption behavior of reactive dye in aqueous solution on chemical cross-linked chitosan beads, Chemosphere 50 (2003) 1095–1105.
[31] Y.S. Ho, G. McKay, Pseudo-second order model for sorption processes, Process Biochem. 34 (1999) 451–465.
[32] V. Vadivelan, K.V. Kumar, Equilibrium, kinetics, mechanism, and process design for the sorption of methylene blue onto rice husk, J. Colloid Interf. Sci. 286 (2005) 90–100.
[33] M.C. Ncibi, B. Mahjoub, M. Seffen, Investigation of the sorption mechanisms of metal-complexed dye onto *Posidonia oceanica* (L.) fibres through kinetic modelling analysis, Bioresour. Technol. 99 (2008) 5582–5589.
[34] V.K. Garg, M. Amita, R. Kumar, R. Gupta, Basic dye (methylene blue) removal from simulated wastewater by adsorption using Indian Rosewood sawdust: a timber industry waste, Dyes Pigments 63 (2004) 243–250.
[35] C. Oktar, L. Yilmaz, H.O. Ozbelge, N. Bicak, Synthesis and characterization of novel silica gel supported N-pyrazole ligand for selective elimination of Hg(II), React. Funct. Polym. 68 (2008) 842.
[36] M.B. McBride, A critique of diffuse double layer models applied to colloid and surface chemistry, Clay Clay Miner. 45 (1997) 598–608.